

Influence of nonlocal chemistry on tracer distributions: Inferring the mean age of air from SF₆

Timothy M. Hall

NASA Goddard Institute for Space Studies, New York

Darryn W. Waugh¹

Cooperative Research Centre for Southern Hemisphere Meteorology, Monash University, Clayton
Victoria, Australia

Abstract. Sulfur hexafluoride (SF₆) is nearly inert in the troposphere and stratosphere and has a documented, steady increase in the troposphere due to industrial sources, making it a useful tracer of atmospheric circulation. Studies using SF₆ to estimate the mean age of stratospheric air have assumed the influence of mesospheric photochemical destruction is negligible. However, the mean age of an air parcel may be sensitive to small fractions of the air that have resided for long times in the upper atmosphere. Here we use two three-dimensional chemical transport models to estimate the influence of mesospheric SF₆ loss on mean age inferences in the stratosphere. Because the mechanisms of SF₆ loss are uncertain, we perform a number of simulations employing a range of magnitudes of a simple constant mesospheric loss frequency, as well as a range of scenarios for SF₆ time variation in the troposphere. Using loss rates producing plausible global lifetimes of SF₆ (1000 to 3000 years), and tropospheric time-variation matching observations, we find that age estimates inferred from SF₆ mixing ratios may be significantly biased and that the bias is increasing in time. For example, the present-day time lag of SF₆ mixing ratio from the troposphere overestimates the mean age by up to 18% at 68°S and 20 km, and up to 65% at 68°S and 30 km, depending on the loss rate and model. Correcting for this bias would bring recent comparisons of modeled and measured mean age closer in line.

1. Introduction

The rate of transport from the troposphere to the stratosphere determines the degree to which pollutants affect stratospheric chemistry. One measure of this transport rate is the mean age Γ , the mean time since a parcel of stratospheric air was last in the troposphere [Hall and Plumb, 1994]. Γ is a timescale independent of any particular chemical tracer. If Γ can be determined from measurements, then models of the stratosphere can have their transport properties assessed independent of chemical computations.

A number of recent observational studies have estimated Γ , using tracers such as CO₂ [Bischof et al., 1985; Schmidt and Khedim, 1991; Boering et al., 1996], CFC-115 [Pollock et al., 1992; Daniel et al., 1996], and

SF₆ [Elkins et al., 1996; Harnisch et al., 1996; Patra et al., 1997]. The technique is as follows: choose a tracer whose tropospheric abundance is increasing, measure its stratospheric mixing ratio, and determine the time lag τ since the troposphere last exhibited that mixing ratio. In order that $\tau = \Gamma$, two criteria must, in principle, be met: (1) the tracer mixing ratio must be linearly varying in time, and (2) the tracer must be inert. In practice, no tracer satisfies either criterion perfectly, and thus τ is an approximation to Γ . Hall and Plumb [1994] discussed the error induced by non-linear time variation. They found that for conserved tracers $\tau \approx \Gamma$ if the time variation was approximately linear over a timescale related to the statistical spread of transit times within an air parcel, which was about 7 years in their model. In general, for a tracer increasing more rapidly than linear, $\tau < \Gamma$.

In this paper, we focus on the bias to estimates of Γ due to chemical loss of the tracer in the upper atmosphere. Several recent studies have used SF₆ to infer Γ (see above references). The advantages of SF₆ are that its surface sources result in a steady increase in atmospheric abundance [Maiss et al., 1996; Geller et al., 1997] (although the increase is not precisely lin-

¹Now at Department of Earth and Planetary Sciences, Johns Hopkins University, Baltimore, Maryland.

Copyright 1998 by the American Geophysical Union.

Paper number 98JD00170.
0148-0227/98/98JD-00170\$09.00

ear, a point to which we return, and which has been addressed by Volk *et al.* [1997]), and that it has apparently no significant in situ chemical loss or production in the troposphere or stratosphere. The photochemistry of SF₆ in the atmosphere is uncertain. Ravishankara *et al.* [1993] estimate that its loss is due primarily to photolysis and electron capture in the mesosphere, leading to a global atmospheric lifetime the order of several thousand years. However, the nature of SF₆ ion chemistry following electron capture is uncertain, and using different assumptions, Morris *et al.* [1995] find a lifetime as low as 800 years. Despite the long global lifetime, the mesospheric loss may be communicated down to the middle and lower stratosphere, altering SF₆ gradients from what they would be due to the tropospheric time variation alone. This causes τ to be greater than what it would be for a perfectly conserved tracer, as one must go further back in the tropospheric record to find a matching value.

We use two chemical transport models (CTMs) driven by winds from two general circulation models (GCMs), and employing an extremely simplified mesospheric loss, to estimate the biases due to nonlinear growth and chemical loss separately and in combination. We estimate the present-day time lag of SF₆ overestimates Γ by up to 18% in the high-latitude lower stratosphere (68°S, 20 km) and up to 65% in the high-latitude middle stratosphere (68°S, 30 km), depending on the loss scenario assumed and the model used. Moreover, the bias is increasing in time. Accounting for such a bias would bring model mean ages closer in line with measurements. (See, for example, the modeled and measured SF₆ comparisons of Waugh *et al.* [1997].) In section 2 we briefly summarize the models and runs, and in section 3 we interpret the results. Appendix A

Table 1. SF₆ Global Lifetime L

n	λ_n	MACCM2	GISS
0	0	∞	∞
1	3×10^{-8}	4761	3528
2	9×10^{-6}	1975	1424
3	3×10^{-7}	861	694
4	3×10^{-6}	293	387

L is in years.

presents a more formal relationship between time lags of nonconserved tracers and the age spectrum, as defined by Hall and Plumb [1994].

2. Chemical Transport Models

We use two three-dimensional off-line chemical transport models (CTMs) driven by different sets of GCM winds to simulate an SF₆-like tracer. One CTM, driven by winds from the National Center for Atmospheric Research Middle Atmosphere version of the Community Climate Model version 2 (NCAR MACCM2), is based on a CTM developed by P. J. Rasch and D. L. Williamson at NCAR [Rasch *et al.*, 1994] and is described in Waugh *et al.* [1997]. We refer to this model as "CCM2." The other CTM, driven by NASA Goddard Institute of Space Studies (GISS) GCM winds, was developed by Michael Prather [Prather *et al.*, 1987; Hall and Prather, 1995]. We refer to it as "GISS." In both cases, we employ a single year of GCM wind data, recycling for multiyear simulations. The two models are quite different, using different advection schemes and resolutions (128×64×44 longitude, latitude, and verti-

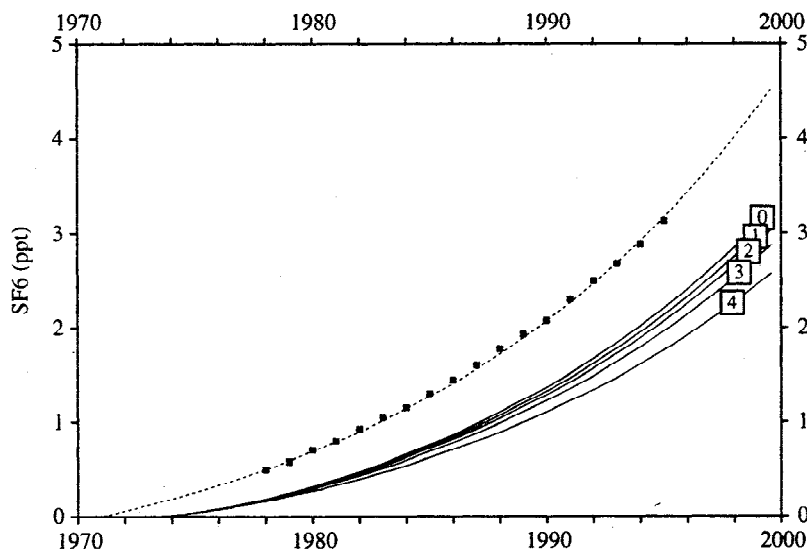


Figure 1. Symbols are surface measurements adapted from Maiss *et al.* [1996]. The dashed curve is an exponential fit to the observations, used as the boundary condition for the CTM. Solid curves are the CCM2 model response at 68°N and 30 km. Different solid curves represent responses assuming different values of mesosphere loss rate for SF₆ and are labeled according to Table 1.

cal levels from the surface to about 80 km for CCM2, and 36×24×21 for GISS over roughly the same domain). We expect to see significant model differences in these experiments. However, as our purpose is to illustrate a sensitivity to a poorly known quantity (SF₆ chemical loss), the model differences can be viewed as a strength of the study. Two quite different models lead to similar conclusions. Note that while the GISS model employed here is the same as in the work of *Hall and Waugh* [1997], the CCM2 is driven by a wind data set from a different NCAR MACCM2 run than in the works of *Hall and Waugh* [1997] and *Waugh et al.* [1997]. Further studies are planned to understand the impact on long-lived tracer distributions to changes in the MACCM2; however, the general conclusions of *Hall and Waugh* [1997] and this study are independent of the version of CCM2. Finally, although the calculations are fully three dimensional, we present only zonally averaged quantities, and all timescales presented are understood to have been averaged about a latitude circle.

3. Simulations

We perform a series of "SF₆" simulations, each employing a different assumed photochemistry scenario. In each simulation, the photochemistry is simple and idealized: SF₆ is lost every model time step at a rate $\lambda\chi$, where χ is the mixing ratio and λ is a loss frequency. The loss frequency has the form

$$\lambda = \begin{cases} 0 & z \leq 60 \text{ km} \\ \lambda_n & z > 60 \text{ km} \end{cases} \quad (1)$$

where λ_n are constants. The different simulations in the series correspond to different values of λ_n , ranging from $\lambda_0 = 0$ (the conserved tracer) to $\lambda_4 = 3 \times 10^{-6} \text{ s}^{-1}$ (see Table 1).

With each λ_n we test a range of tropospheric growth scenarios. This may be done with only a single simulation per loss scenario by computing the Green's function $G(\mathbf{x}, t)$ of the CTM. The Green's functions are calculated in the same manner as in the works of *Hall and Plumb* [1994] and *Hall and Waugh* [1997]. Given $G(\mathbf{x}, t)$, the tracer response $\chi(\mathbf{x}, t)$ at \mathbf{x} to any tropospheric mixing ratio history $\chi(0, t)$ can be obtained by convolving $G(\mathbf{x}, t)$ with $\chi(0, t)$ (see Appendix A for details). Here we consider the case of tropospheric mixing ratios that increase exponentially with time; that is,

$$\chi(0, t) = \begin{cases} 0 & t < t_0 \\ \chi_0(e^{(t-t_0)/T} - 1) & t \geq t_0 \end{cases} \quad (2)$$

The timescale T defines the growth scenario. Note that $T = 16$ years (with $\chi_0 = 0.91$ ppt and $t_0 = 1971$) fits well the observed surface SF₆ time series of *Maiss et al.* [1996] (see Figure 1). As $T \rightarrow \infty$, the growth approaches linear.

Convolution of $\chi(0, t)$ with $G(\mathbf{x}, t)$ is equivalent to a simulation having a time-dependent boundary condition on the mixing ratio of $\chi(0, t)$. Although a boundary condition on the mixing ratio near the surface is

not as physical as a boundary condition on the flux out of the surface, it allows use of measurements of SF₆ mixing ratios, which are not available for fluxes. It is worth noting here why the use of a mixing ratio boundary condition results in little error compared to a flux boundary condition. As a relevant example, consider surface boundary conditions of a constant flux and a linearly increasing mixing ratio. For a conserved tracer, the two boundary conditions result in nearly identical atmospheric simulations: in either case, following an initial transient state of several years, the entire atmosphere displays a mixing ratio increasing linearly at the same rate. This equivalence of boundary condition form does not, in general, hold for tracers undergoing photochemical loss. For such tracers, a constant flux boundary condition eventually results in a steady state (in an

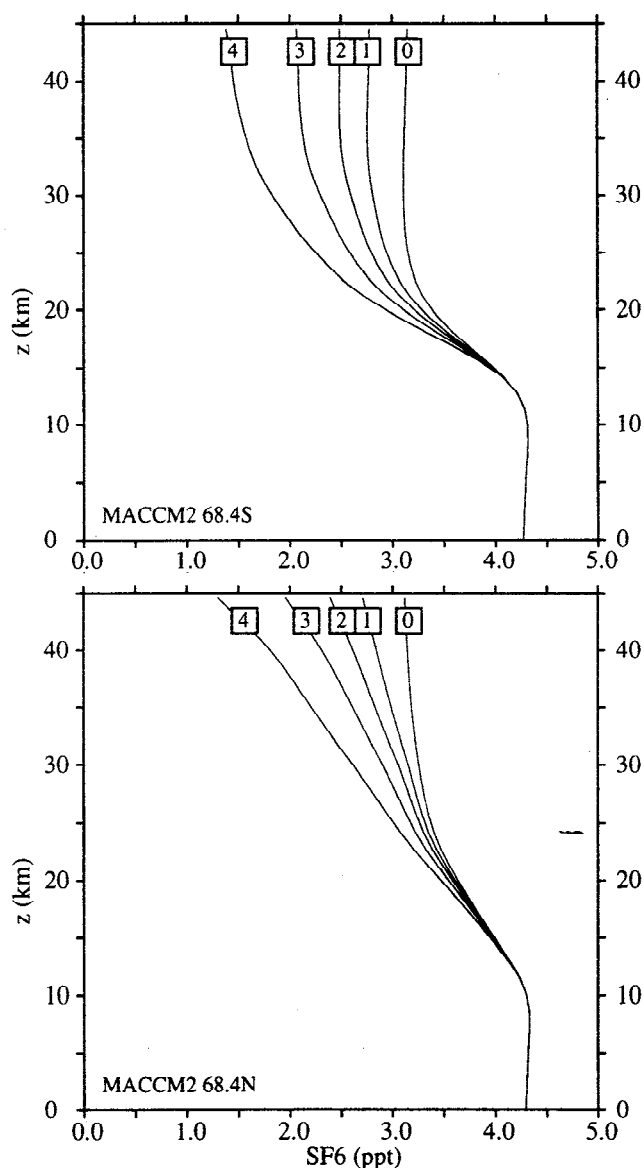


Figure 2. Profiles of SF₆ at (top) 68°S and (bottom) 68°N in CCM2. The different curves represent different loss scenarios, with the labels corresponding to those of Table 1.

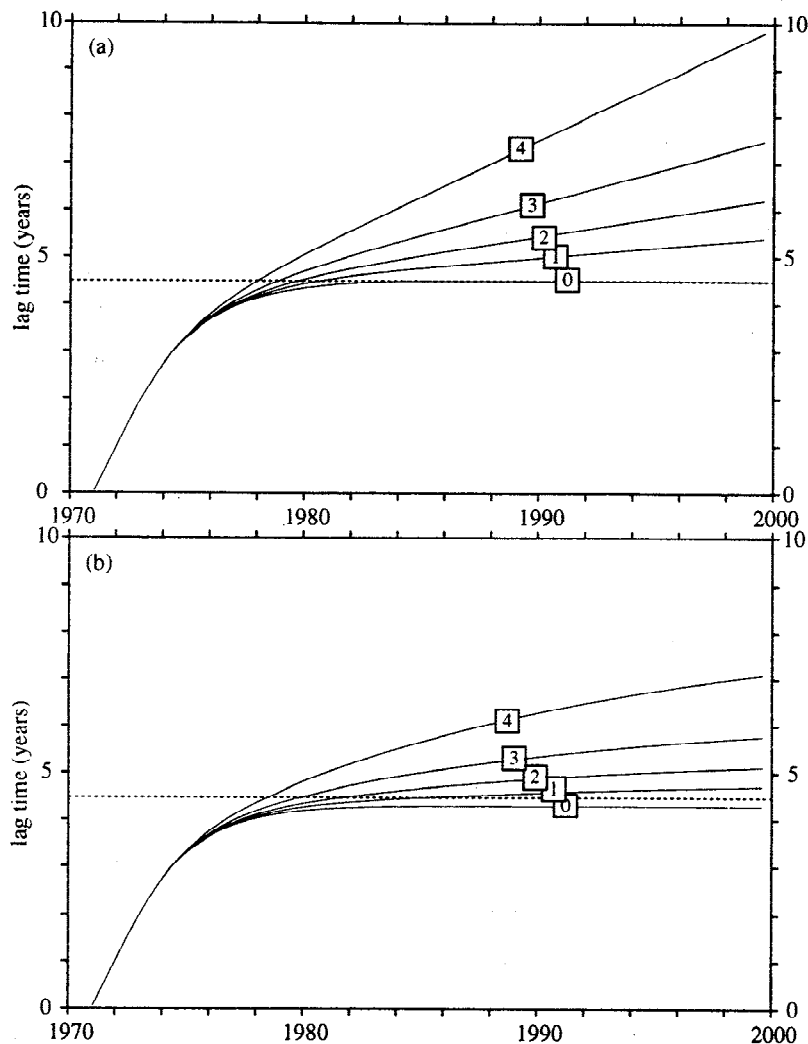


Figure 3. The time lag τ as a function of time from initialization for the CCM2 at 68.4°N and 30 km. (a) A linearly increasing boundary condition, and (b) the exponential boundary condition fit to observed SF₆ (shown in Figure 1). The horizontal dashed line indicates the value of Γ . The solid lines are τ for different assumed values of loss rate in the mesosphere and are labeled according to Table 1.

annually averaged sense, for a CTM recycling a single year of wind data), in which the surface source balances the loss aloft. A simulation having a mixing ratio boundary condition can never achieve a steady state, as the tracer always increases in the boundary condition region, by definition. However, for the tracers simulated here, this is not a significant issue. As discussed in Appendix B, the time for the flux boundary condition to achieve its steady state is the global chemical lifetime L of the tracer, several hundreds to thousands of years for these SF₆-like tracers (see Table 1). Because we simulate only several decades, to a good approximation, a boundary condition on the mixing ratio suffices.

4. Results

Figure 1 shows the surface time series of SF₆ and the responses of CCM2 to this surface variation in the high-latitude middle stratosphere (68°N, 30 km) for

different loss scenarios. The symbols, adapted from the measurements of Maiss *et al.* [1996], are fit with exponential form (2) using $\chi_0 = 0.9$ ppt, $t_0 = 1971$, and $T = 16$ years, which is shown as a dashed line in the figure, while the responses at 68°N and 30 km are shown as solid lines in the figure for varying λ_n . (Responses are labeled by n , as in Table 1.) Although, like the tropospheric variation, the tracer responses in the stratosphere are also exponential, the shorter the chemical lifetime, the slower the exponential increase (see Appendix A for details). Vertical profiles at high latitudes for the year 1998 are shown in Figure 2 for the different loss scenarios.

Figure 3 shows the time lag τ of CCM2 as a function of time at 68°N and 30 km for tracers of various chemical lifetimes and linear tropospheric increase (Figure 3a), and tracers of the same lifetimes, but exponential tropospheric increase (Figure 3b), as shown in Figure 1. Here $\Gamma = 4.49$ years, as indicated by the dashed hor-

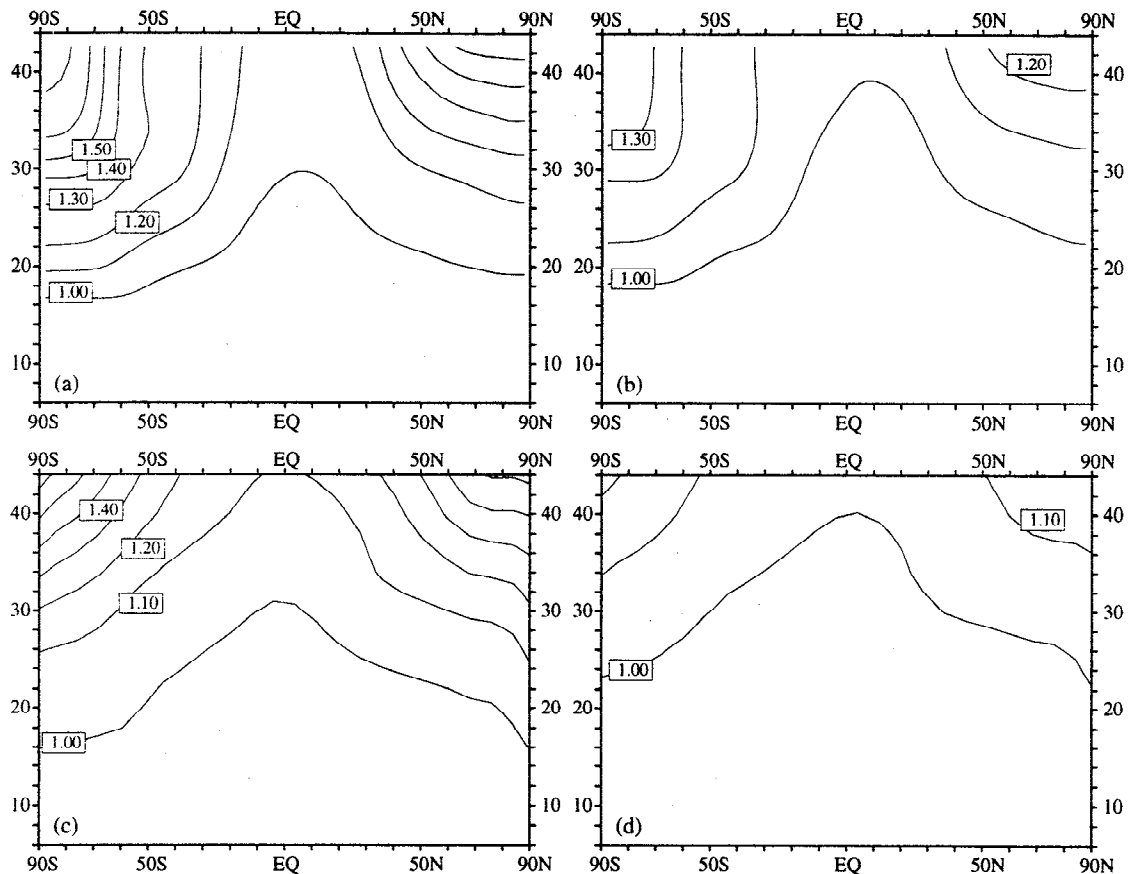


Figure 4. The ratio τ/Γ versus latitude and height for the year 1998. (a) CCM2 and λ_2 ; (b) CCM2 with λ_1 ; (c) GISS with λ_2 ; and (d) GISS with λ_1 .

horizontal line. Focus first on the purely linear tracer. After about 12 years, τ_0 (the lag of the conserved tracer) converges to Γ . Conserved tracers increasing linearly in time yield Γ as their lag time [Hall and Plumb, 1994]. On the other hand, τ_1 through τ_4 , the lags for tracers with mesospheric loss, never converge; following the 12 year transient period, they assume a linear increase whose rate depends on λ_n (see Appendix A for the mathematical statement). With loss aloft, the atmosphere cannot keep pace with the linear increase in the troposphere.

The τ for the exponentially increasing tracers are complicated by additional effects. For conserved tracers, exponential increase results in a time lag less than the mean age [Hall and Plumb, 1994]: as seen in Figure 3b, after 12 years, $\tau_0 = 0.94\Gamma$. The nonconserved tracers, following the initial transience, assume a state in which they asymptote, after time T , to constant values dependent on the particular λ_n . Thus the τ overestimate of Γ due to photochemical loss aloft is partially offset by the effects of nonlinear increase in the troposphere. In Appendix A, this is stated more formally, and the linear behavior is shown to be the limiting case of the exponential behavior.

Figure 4 shows the spatial distribution of τ_1/Γ and τ_2/Γ in the year 1998 for CCM2 and GISS, using the exponential tropospheric increase with $T = 16$ years

(see Table 1 for the corresponding global photochemical lifetimes L). The τ/Γ contours bulge up in the tropics and slope down toward either pole. In the troposphere and parts of the tropical stratosphere, $\tau < \Gamma$; in these regions, the tendency for mesospheric loss to increase τ is more than offset by the tendency for the nonlinear tropospheric growth to decrease τ . However, throughout the extratropical stratosphere, the photochemical loss effect dominates, and $\tau > \Gamma$. Latitudinal gradients are particularly steep in CCM2, and this model shows the largest τ/Γ . High latitudes are regions of downwelling, where air photochemically depleted of SF₆ descends from the mesosphere.

In the high-latitude southern hemisphere of CCM2, the τ_2 overestimate of Γ is up to 50% in the middle stratosphere, although it is much smaller in the lower stratosphere and in the northern hemisphere. Compared to CCM2, GISS has less steep latitudinal gradients, as it does not isolate the tropics from midlatitudes and midlatitudes from the polar vortex as completely. For GISS, τ/Γ is everywhere smaller than for CCM2. For both models, the Γ overestimation by τ_1 (longer global lifetime) is much smaller than by τ_2 (shorter global lifetime).

In order to examine further the relative effects of nonlinear growth and photochemical loss, we test the sensitivity of τ/Γ to T and L (through λ_n) separately. Fig-

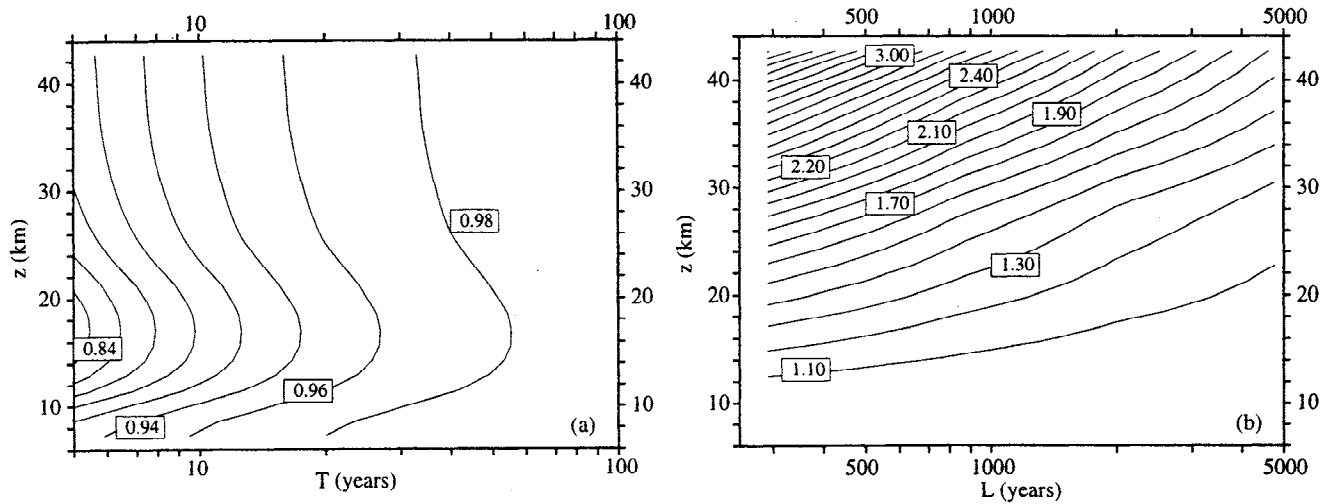


Figure 5. The ratio τ/Γ versus altitude and (a) T and (b) L . The model used is CCM2, and the latitude is 68°N .

ure 5a shows the variation of τ_0/Γ with height and T at high latitudes (68°N) for CCM2. Everywhere $\tau_0/\Gamma < 1$, although it asymptotes to 1 at each height as $T \rightarrow \infty$; that is, as the growth tends to linear, the lag time approaches the mean age. The nonlinear growth effect

is small for realistic T . For example, $\tau_0/\Gamma \approx 0.9$ in the lower stratosphere for $T = 10$ years. Note that the lower stratosphere displays the largest nonlinear growth effect. *Hall and Plumb [1994]* showed that in order for $\tau_0/\Gamma \approx 1$, the constraint on the growth rate

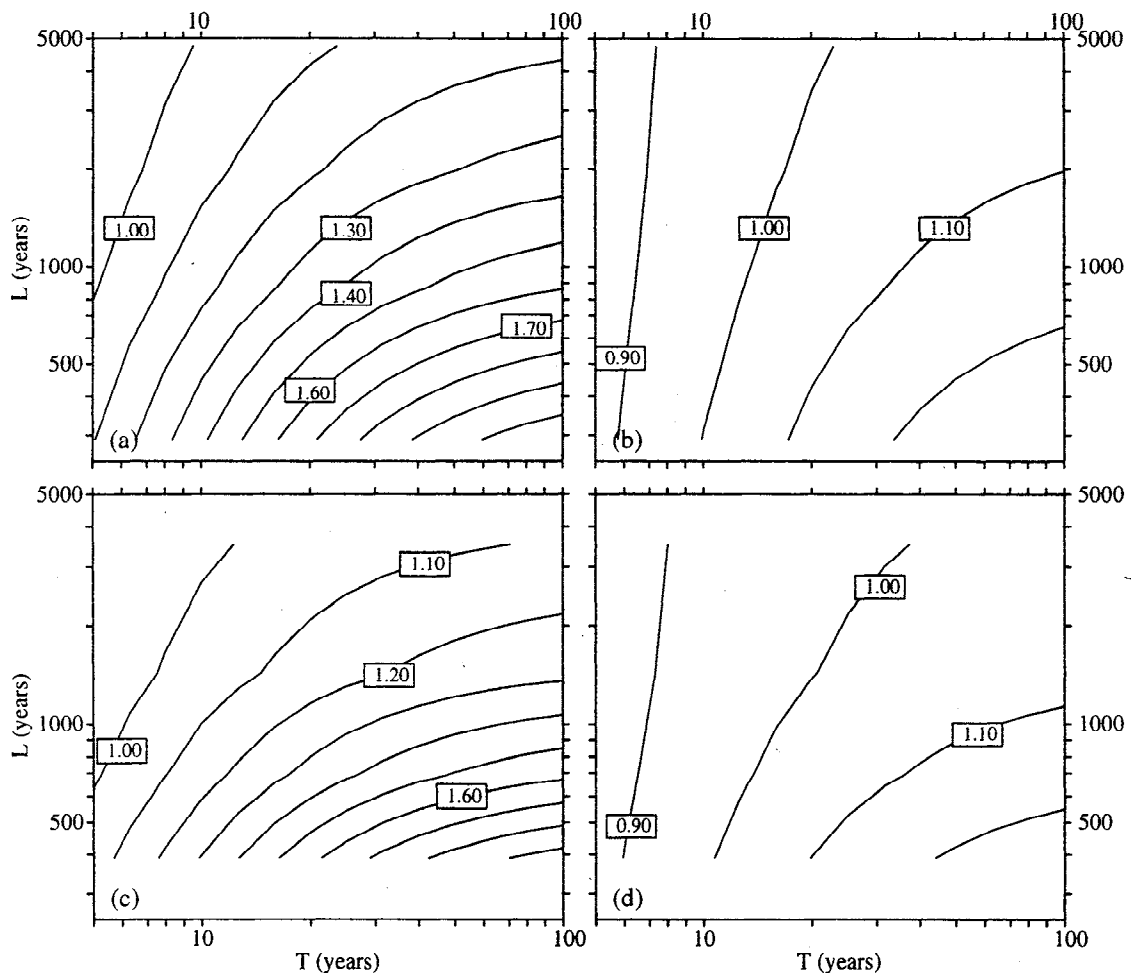


Figure 6. The ratio τ/Γ contoured as a function of L (vertical axes) and T (horizontal axes); (a) CCM2 at 68°N and 30 km; (b) CCM2 at 43°N and 20 km; (c) GISS at 67°N and 30 km; and (d) GISS at 43°N and 20 km.

Table 2. Range of τ/Γ for $L = 3000\text{--}1000$ Years

	20 km (CCM2)	20 km (GISS)	30 km (CCM2)	30 km (GISS)
68°N	1.00–1.05	0.96–1.02	1.11–1.27	1.03–1.20
43°N	0.98–1.02	0.95–1.00	1.06–1.18	1.01–1.14
43°S	1.01–1.07	0.96–1.01	1.18–1.40	1.00–1.10
68°S	1.07–1.18	0.98–1.05	1.32–1.65	1.06–1.22

is $T \gg \Delta^2/\Gamma$, where Δ is the “age spectral width,” a measure of the statistical spread of transit times contained in a stratospheric air parcel. For GISS and CCM2, Δ^2/Γ has a weak maximum with height in the lower stratosphere at high latitudes, as shown in the GISS model by *Hall and Plumb* [1994].

Figure 5b shows the variation of τ/Γ with height and $\log L$ for a linearly increasing tropospheric mixing ratio, again at high latitudes and for CCM2. The figure is generated by interpolating results from the five CCM2 simulations. For a given lifetime, the τ overestimate of Γ increases with height, that is, stratospheric regions closest to the loss (which starts at 60 km) are most affected. For a given height, with increasing L , τ converges to Γ .

The combined effects of loss and nonlinear growth are shown by contouring τ/Γ versus L and T for CCM2 and GISS at 68°N and 30 km (Figure 6a and 6c) and 43°N and 20 km (Figures 6b and 6d). For fixed T , the τ overestimate of Γ decreases with increasing L , while for fixed L , it increases with T . Using the SF₆ lifetimes of 3000 to 1000 years based on the analyses of *Ravishankara et al.* [1993] and *Morris et al.* [1995], we find the range of τ/Γ shown in Table 2. In the lower stratosphere, the loss effect for the longer lifetimes is small enough to be completely compensated by the nonlinear growth effect. Closer to the loss region the loss effect dominates.

Our conclusions are not sensitive to reasonable assumptions about the location of SF₆ photochemical loss. Figure 7 displays plots as in Figure 6c, except that the height of onset of SF₆ loss in GISS has been raised: in Figure 7a the loss occurs only above 72 km (the top two model levels), and in Figure 7b the loss occurs only above 80 km (the top one model level). Note that the extent of L coverage varies somewhat. For each onset altitude, we performed several simulations using λ_n values from Table 1, as well as additional λ_n , so that the resulting range of L would roughly match that of Figure 6. There is relatively little variation in τ/Γ from onset altitudes 60 km to 72 km to 80 km. For example, at $T = 16$ years and $L = 2000$ years, τ/Γ varies from 1.07 for an onset of 60 km to 1.06 for an onset of 80 km.

This insensitivity to the location of the loss region suggests that the model mesosphere is rapidly mixed compared to vertical transport in the stratosphere. The extra time to transport chemical loss to the middle stratosphere from 80 km compared to transporting from 60 km is smaller than the time to transport new tracer from the troposphere to middle stratosphere. This ob-

servation is born out in Γ as well: both GISS and CCM2 have vertical Γ gradients larger in the lower stratosphere than aloft [*Hall and Waugh*, 1997]. In the extreme limit of instantaneous mesospheric mixing, there are no SF₆ gradients in the region, and L and τ/Γ are independent of the location of the loss region within the mesosphere. This limit represent a lower bound on L for a given loss rate λ . For example, by assuming instantaneous mixing above 50 km, *Ravishankara et al.* [1993] found a lower bound of L about 5.5 times smaller than their best esti-

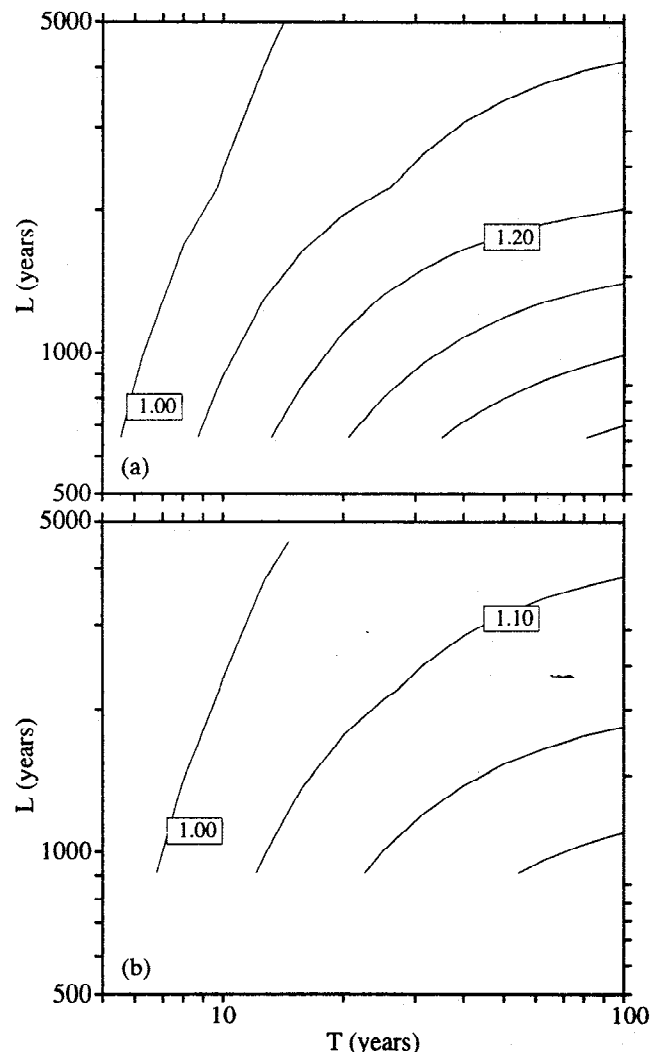


Figure 7. As in Figure 6c, but with varying altitude of onset for chemical loss in GISS: (a) loss occurs above 72 km (top two model levels); (b) loss occurs above 80 km (top one level of model).

mate value (3200 years). On the other hand, if vertical mixing in the mesosphere is slower than occurs in GISS and CCM2, L is larger for a given λ , and τ/Γ is more sensitive to loss location.

5. Discussion and Summary

We have used two CTMs to examine the impact of mesospheric loss on the inference of Γ from SF₆ observations. Assuming SF₆ is conserved may lead to overestimates of mean age up to 65% in the high-latitude middle stratosphere (68°S, 30 km), depending on the loss scenario and the CTM, although the effect at mid-latitudes in the lower stratosphere is much smaller. Accounting for such a bias would bring previously noted discrepancies of modeled and measured mean age closer in line. For example, the high-latitude Γ estimates of up to 10 years by *Harnisch et al.* [1996] are close to the modeled Γ of *Waugh et al.* [1997] when reduced by 30%.

The sensitivity of Γ estimates to SF₆ loss in the mesosphere may at first seem surprising. However, Γ of an air parcel is a mean over a spectrum of transit times of irriducible fluid elements within the parcel. Thus, although only a small fraction of air in a stratospheric parcel may have traversed the mesosphere, these elements have, in general, the longest transit times and therefore most heavily contribute to Γ . The details of SF₆ photochemistry are not well quantified, and thus it seems unlikely that we can accurately correct the bias this photochemistry introduces to Γ estimates. Therefore, if $\tau/\Gamma \approx 1.1$ is realistic in the high-latitude lower stratosphere, for example, this may indicate Γ can never be inferred more accurately than 10% from SF₆ (or indeed from any tracer, since it is hard to imagine identifying a better suited age tracer than SF₆). Nonetheless, 10% is still smaller than the difference between most models and measurements. Therefore SF₆ measurements can still provide a valuable constraint on the transport of models, particularly below the middle stratosphere. In the middle and upper stratosphere, however, the uncertainty of SF₆ mesospheric loss rates may prevent its observations from tightly constraining models.

Appendix A: Age Spectral Description

The age spectral formalism of *Hall and Plumb* [1994] can be extended to include chemical loss processes. Consider a trace gas of mixing ratio $\chi(\mathbf{x}, t)$ with surface source and upper atmosphere loss. The response at some point in the middle atmosphere to a tropospheric time variation $\chi(0, t)$ is

$$\chi(\mathbf{x}, t) = \int_0^t \chi(0, t-t') G_\lambda(\mathbf{x}, t') dt' \quad (\text{A1})$$

$G_\lambda(\mathbf{x}, t')$ is the Green's function at position \mathbf{x} and time $t' < t$ (we assume stationary transport, so that G_λ is independent of t); the subscript λ indicates the presence of chemical loss. The "loss spectrum" is defined as $L_\lambda(\mathbf{x}, t) = G_\lambda(\mathbf{x}, t)/G(\mathbf{x}, t)$, where $G(\mathbf{x}, t)$ is the age

spectrum; that is, the Green's function for a conserved tracer ($\lambda = 0$ for all \mathbf{x}). $L_\lambda(\mathbf{x}, t)$ represents the fractional chemical loss of tracer having transit time t [*Volk et al.*, 1997]. Note that $L_\lambda(\mathbf{x}, t) \leq 1$ for all \mathbf{x} and t .

$G(\mathbf{x}, t)$ and $1 - L_\lambda(\mathbf{x}, t)$ of GISS and CCM2 are plotted for several altitudes at high latitudes in Figure A1, using $\lambda_n = \lambda_2$ (see Table 1). Note that $L_\lambda(\mathbf{x}, t) < 1$ even in regions \mathbf{x} where the local chemical loss rate is zero. Information of chemical loss in remote regions is communicated by transport. For a tracer having surface source and mesospheric loss, we expect $L_\lambda(\mathbf{x}, t)$ in the lower stratosphere to decrease with increasing transit time t . Air that has come directly to \mathbf{x} from the troposphere, and thus has undergone no chemical loss, has predominantly short transit times. On the other hand, a significant fraction of air that has traversed the mesosphere and been depleted of χ before arriving at \mathbf{x} has long transit times. Note that the high-latitude downwelling, which transports SF₆-depleted air from the mesosphere to lower levels, is strongly seasonal, explaining the annual cycle seen in $L_\lambda(\mathbf{x}, t)$.

Consider a tropospheric time dependence given by (2). The stratospheric response, according to (A1), is

$$\begin{aligned} \chi(\mathbf{x}, t) &= \chi_0 e^{-(t-t_0)/T} \int_0^t e^{-t'/T} L_\lambda(\mathbf{x}, t') G(\mathbf{x}, t') dt' \\ &\quad - \chi_0 \int_0^t L_\lambda(\mathbf{x}, t') G(\mathbf{x}, t) dt' \end{aligned} \quad (\text{A2})$$

where we have used the definition of $L_\lambda(\mathbf{x}, t)$. Following a transience whose duration depends on $G(\mathbf{x}, t)$ (less than 10 years for these models), but not on the nature of $\chi(0, t)$, the integration bounds in (A2) may be taken to infinity. Thus $\chi(\mathbf{x}, t) \propto e^{t'/T}$, but with an offset and multiplying coefficient dependent on the loss scenario.

In order to estimate $\Gamma(\mathbf{x})$, $\tau(\mathbf{x})$ is found such that $\chi(\mathbf{x}, t) = \chi(0, t - \tau(\mathbf{x}))$. Substituting $\chi(0, t - \tau(\mathbf{x}))$ with (2) for the left-hand side of (A2) and solving for $\tau(\mathbf{x})$ gives

$$\begin{aligned} \tau(\mathbf{x}, t) &= -T \ln \left(\int_0^\infty e^{-t'/T} L_\lambda(\mathbf{x}, t') G(\mathbf{x}, t') dt' \right. \\ &\quad \left. + e^{-(t-t_0)/T} \left(1 - \int_0^\infty L_\lambda(\mathbf{x}, t') G(\mathbf{x}, t') dt' \right) \right) \end{aligned} \quad (\text{A3})$$

First, consider the limit of no chemical loss, in which case, $L(\mathbf{x}, t) = 1$ for all \mathbf{x} and t ; $\int_0^\infty G(\mathbf{x}, t) dt = 1$ [*Hall and Plumb*, 1994], so that the second term on the right of (A3) vanishes, leaving

$$\tau(\mathbf{x}) = -T \ln \left(\int_0^\infty e^{-t'/T} G(\mathbf{x}, t) dt \right) \quad (\text{A4})$$

a result independent of time. *Hall and Plumb* [1994] showed that (A4) becomes $\tau(\mathbf{x}) \sim \Gamma(\mathbf{x})$ for $T \gg \Delta^2/\Gamma$, where Δ is the width of the age spectrum ($\Delta^2/\Gamma \approx 1.5$ years for CCM2, with little spatial variation). Thus, for a conserved tracer undergoing a surface increase approximately linear over a timescale of several years or more, and after an initial transience whose duration is independent of the rate of increase, the stratospheric lag time of the tracer approximates the mean age. This is the case illustrated by τ_0 in Figure 3b.

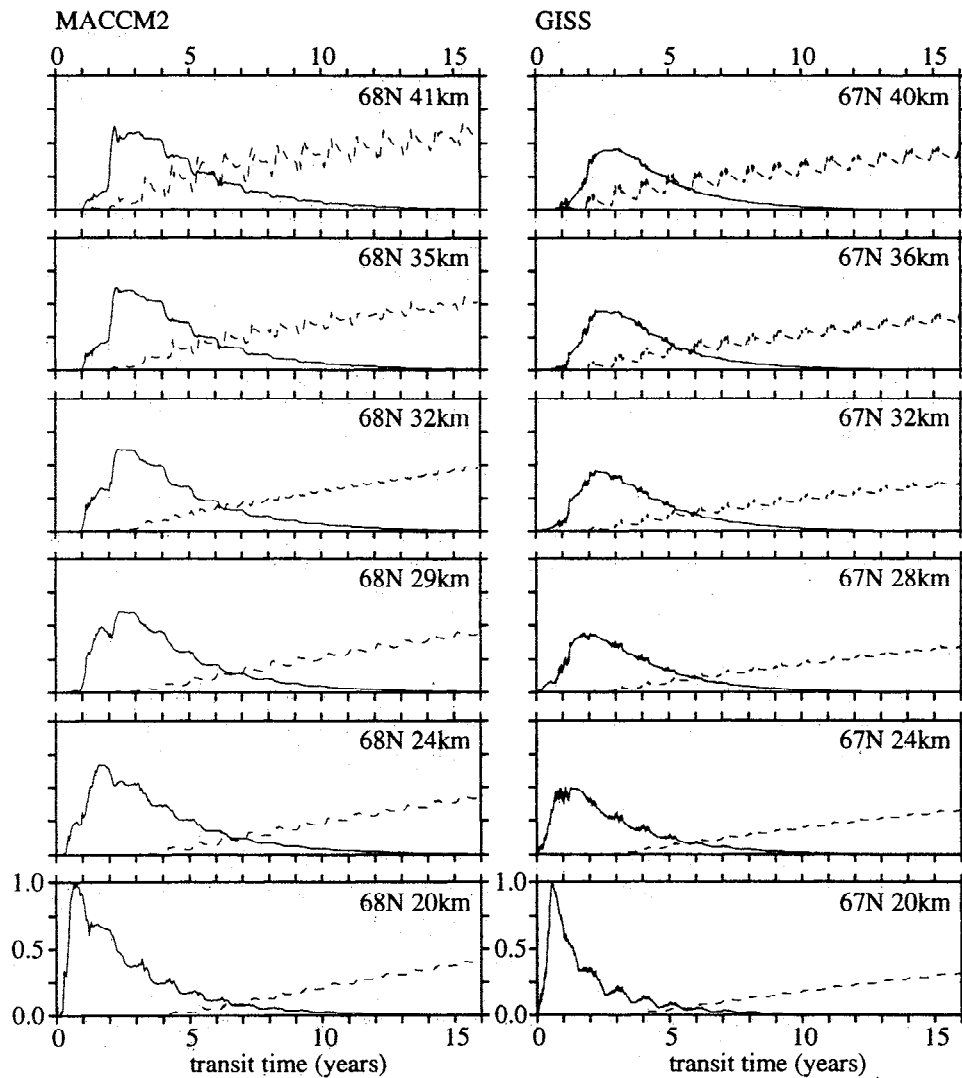


Figure A1. Age spectra (solid curves) and loss spectra (dashed curves) at heights and latitudes as labeled. The left column is CCM2, and the right column is GISS. The horizontal axis is transit time, while the vertical, referring to the loss spectra, is fractional loss from 0 to 1. The age spectra have been normalized to peak at 1 at the bottom level plotted for each model.

More generally, the second term on the right of equation (A3) does not vanish. Only for $t \gg T$ is it negligible. In other words, a steady lag time exists only following a second transient period (in addition to the first transient determined exclusively by $G(\mathbf{x}, t)$), whose duration depends explicitly on the nature of the time-dependent boundary condition.

If the tracer χ has purely linear time variation in the forcing region, then (A4) becomes $\tau(\mathbf{x}) = \Gamma(\mathbf{x})$, if χ is conserved. For the case with chemical loss, the linear result is found by substituting the large T limit of (2) into (A1), yielding

$$\begin{aligned} \tau(\mathbf{x}) \sim & \int_0^\infty t' L_\lambda(\mathbf{x}, t') G(\mathbf{x}, t') dt' \\ & + (t - t_0) \left(1 - \int_0^\infty L_\lambda(\mathbf{x}, t') G(\mathbf{x}, t') dt \right) \end{aligned} \quad (\text{A5})$$

The stratospheric lag increases linearly with time at each location, the case shown by τ_0 in Figure 3a.

Appendix B: Flux Form Boundary Conditions

We show here that a constituent having constant mass flux from the surface and atmospheric chemical loss proportional to mixing ratio achieves a steady state in a time equal to its global chemical lifetime. Consider the tracer continuity equation for the mixing ratio χ :

$$\frac{\partial}{\partial t} \chi + \mathcal{L}(\chi) = -\lambda(\mathbf{x})\chi \quad (\text{B1})$$

with a boundary condition of tracer flux F_χ out of the surface. \mathcal{L} is a linear transport operator. Integrating (B1) over the mass of the atmosphere yields

$$\frac{\partial}{\partial t} M_\chi - F_\chi = -\frac{1}{L} M_\chi \quad (\text{B2})$$

where M_χ is the total tracer mass in the atmosphere, L is the global chemical lifetime, defined by the integral over the atmosphere

$$L^{-1} = \frac{1}{M_{\chi}} \int \lambda(\mathbf{x}) \chi(\mathbf{x}) \rho(\mathbf{x}) d\mathbf{x} \quad (\text{B3})$$

and $\rho(\mathbf{x})$ is the density of air. To obtain (B2) from (B1), we use the fact that the integral of $\mathcal{L}(\chi)$ over the entire domain must equal the net flux out of the domain, which in this case is $-F_{\chi}$. (The negative sign indicates that upward flux from the surface is flux into the domain.)

Equation (B2) for the total tracer mass has the solution

$$M_{\chi}(t) = F_{\chi} L (1 - e^{-t/L}) \quad (\text{B4})$$

In other words, the steady state $F_{\chi} L$ is achieved after a transient of duration L . Note that for $t \ll L$ (the case for all the simulations considered in this study),

$$M_{\chi}(t) \sim F_{\chi} t \quad (\text{B5})$$

The total tracer mass increases linearly in time.

Acknowledgments. Most of this research was conducted while T.M.H. was a fellow at the Cooperative Research Centre for Southern Hemisphere Meteorology, Clayton, Australia. The center is supported through the Australian Government Cooperative Research Centre Program.

References

- Bischof, W., R. Borchers, P. Fabian, and B. C. Kruger, Increased concentration and vertical distribution of carbon dioxide in the stratosphere, *Nature*, **316**, 708-710, 1985.
- Boering, K. A., S. C. Wofsy, B. C. Daube, H. R. Schneider, M. Loewenstein, and J. R. Podolske, Stratospheric transport rates and mean age distribution derived from observations of atmospheric CO₂ and N₂O, *Science*, **274**, 1340-1343, 1996.
- Daniel, J. S., S. M. Schauffler, W. H. Pollack, S. Solomon, A. Weaver, L. E. Heidt, R. R. Garcia, E. L. Atlas, and J. F. Vedder, On the age of stratospheric air and inorganic chlorine and bromine release, *J. Geophys. Res.*, **101**, 16,757-16,770, 1996.
- Elkins, J. W., et al., Airborne gas chromatograph for in situ measurements of long-lived species in the upper troposphere and lower stratosphere, *Geophys. Res. Lett.*, **23**, 347-350, 1996.
- Geller, L. S., J. W. Elkins, R. C. Myers, J. M. Lobert, A. D. Clarke, D. H. Hurst, and J. H. Butler, Tropospheric SF₆: Observed latitudinal distribution and trends, derived emissions, and interhemispheric exchange time, *Geophys. Res. Lett.*, **24**, 675-678, 1997.
- Hall, T. M., and R. A. Plumb, Age as a diagnostic of stratospheric transport, *J. Geophys. Res.*, **99**, 1059-1070, 1994.
- Hall, T. M., and M. J. Prather, Seasonal evolutions of N₂O, O₃, and CO₂: Three-dimensional simulations of stratospheric correlations, *J. Geophys. Res.*, **100**, 16,699-16,720, 1995.
- Hall, T. M., and D. W. Waugh, Timescales for the stratospheric circulation derived from tracers, *J. Geophys. Res.*, **102**, 8991-9001, 1997.
- Harnisch, J., R. Borchers, P. Fabian, and M. Maiss, Tropospheric trends for CF₄ and C₂F₆ since 1982 derived from SF₆ dated stratospheric air, *Geophys. Res. Lett.*, **23**, 1099-1102, 1996.
- Maiss, M., L. P. Steele, R. J. Francey, P. J. Fraser, R. L. Langenfelds, N. B. A. Trivett, and I. Levin, Sulfer hexafluoride: A powerful new atmospheric tracer, *Atmos. Environ.*, **30**, 1621-1629, 1996.
- Morris, R. A., T. M. Miller, A. A. Viggiano, J. F. Paulson, S. Solomon, and G. Reid, Effects of electron and ion reactions on atmospheric lifetimes of fully fluorinated compounds, *J. Geophys. Res.*, **100**, 1287-1294, 1995.
- Patra, P. K., S. Lal, B. H. Subbaraya, C. H. Jackman, and P. Rajaratnam, Observed vertical profile of sulphur hexafluoride (SF₆) and its atmospheric applications, *J. Geophys. Res.*, **102**, 8855-8859, 1997.
- Pollock, W. A., L. E. Heidt, R. A. Lueb, J. F. Vedder, M. J. Mills, and S. Solomon, On the age of stratospheric air and ozone depletion potentials in the polar regions, *J. Geophys. Res.*, **97**, 12,993-12,999, 1992.
- Prather, M. J., M. B. McElroy, S. C. Wofsy, G. Russell, and D. Rind, Chemistry of the global troposphere: Fluorocarbons as tracers of air motion, *J. Geophys. Res.*, **92**, 6579-6613, 1987.
- Rasch, P. J., X. Tie, B. A. Boville, and D. L. Williamson, A three-dimensional transport model for the middle atmosphere, *J. Geophys. Res.*, **99**, 999-1017, 1994.
- Ravishankara, A. R., S. Solomon, A. A. Turnipseed, and R. F. Warren, Atmospheric lifetimes of long-lived halogenated species, *Science*, **259**, 194-199, 1993.
- Schmidt, U., and A. Khedim, In situ measurements of carbon dioxide in the winter arctic vortex and at midlatitudes: An indicator of the age of stratospheric air, *Geophys. Res. Lett.*, **18**, 763-766, 1991.
- Volk, C. M., J. W. Elkins, D. W. Fahey, G. S. Dutton, J. M. Gilligan, M. Loewenstein, P. R. Podolske, K. R. Chan, and M. R. Gunson, Evaluation of source gas lifetimes from stratospheric observations, *J. Geophys. Res.*, **102**, 25,543-25,564, 1997.
- Waugh, D. W., et al., Three-dimensional simulations of long-lived tracers using winds from MACCM2, *J. Geophys. Res.*, **102**, 21,493-21,513, 1997.

T. M. Hall, NASA Goddard Institute for Space Studies, 2880 Broadway, New York, NY 10025. (e-mail: thall@giss.nasa.gov)

D. W. Waugh, Department of Earth and Planetary Science, The Johns Hopkins University, 3400 N. Charles St., Baltimore, MD 21218. (e-mail: waugh@jhu.edu)

(Received October 22, 1997; revised January 2, 1998; accepted January 9, 1998.)